Pancreatic hyperplasia after gastric bypass surgery in a GK rat model of non-obese type 2 diabetes

Xinrong Zhou[1], Bangguo Qian[2,3], Ning Ji[2,4], Conghui Lui[2], Zhiyuan Liu[2], Bing Li[2], Huarong Zhou[2,5,6] and Caifeng Yan[4]

[1]Department of Endocrinology, Tongji Hospital, Wuhan 430030, China
[2]Key Laboratory of Systems Biology, Institute of Biochemistry and Cell Biology, Chinese Academy of Sciences, Shanghai 200031, China
[3]Pathology Core Facility Institute, Pasteur of Shanghai Chinese Academy of Science, 320 Yueyang Road, Shanghai 200031, China
[4]Clinical Medical College of Yangzhou University, Yangzhou, Jiangsu 225001, China
[5]Jiangsu University, Zhenjiang, Jiangsu 212013, China
[6]Sherman College of Chiropractic, Boiling Springs, South Carolina 29316, USA

Correspondence should be addressed to H Zhou or C Yan
Emails
huarongzhou@hotmail.com or jojohr9@qq.com

Abstract

Gastric bypass surgery produces clear antidiabetic effects in a substantial proportion of morbidly obese patients. In view of the recent trend away from 'bariatric' surgery and toward 'metabolic' surgery, it is important to elucidate the enhancing effect of bypass surgery on pancreatic β-cell mass, which is related to diabetes remission in non-obese patients. We investigated the effects of gastric bypass surgery on glycemic control and other pancreatic changes in a spontaneous non-obese type 2 diabetes Goto-Kakizaki rat model. Significant improvements in postprandial hyperglycemia and plasma c-peptide level were observed when glucose was administered orally post-surgery. Other important events observed after surgery were enhanced first phase insulin secretion in a *in site* pancreatic perfusion experiment, pancreatic hyperplasia, improved islet structure (revealed by immunohistochemical analysis), striking increase in β-cell mass, slight increase in ratio of β-cell area to total pancreas area, and increased number of small islets closely related to exocrine ducts. No notable changes were observed in ratio of β-cell to non-β endocrine cell area, β-cell apoptosis, or β-cell proliferation. These findings demonstrate that gastric bypass surgery in this rat model increases endocrine cells and pancreatic hyperplasia, and reflect the important role of the gastrointestinal system in regulation of metabolism.

Key Words
- type 2 diabetes mellitus
- gastric bypass surgery
- β-cell
- hyperplasia

Journal of Endocrinology (2016) **228**, 13–23

Journal of Endocrinology

Introduction

There is an increasing need for effective medical treatment of type 2 diabetes mellitus (T2DM) because the number of cases worldwide are growing fast and conventional therapeutic strategies have only limited efficacy. Bariatric surgery is often used to treat morbid obesity (BMI >39), and has a notable effect in resolving T2DM in these obese patients (Pories *et al.* 1995, Schauer *et al.* 2003, Khoo *et al.* 2014). Roux-en-Y gastric bypass (RYGB), the most common type of bariatric surgery, converts ~82% of diabetic obese patients and 100% of prediabetic obese patients to normal status (Schauer *et al.* 2000, Wittgrove & Clark 2000). Long-term follow-up studies showed

http://joe.endocrinology-journals.org
DOI: 10.1530/JOE-14-0701

Published by Bioscientifica Ltd.

that good plasma glucose (PG) and HbA1C levels were sustained for decades following discontinuation of all diabetes-related medications (Pories *et al*. 1995). Biliopancreatic diversion and duodenal switch surgery were even more effective for diabetes control (98–100% resolution of T2DM). However, they are more difficult to perform and lead to nutritional problems (Scopinaro *et al*. 1996).

The ability of bariatric surgery to resolve T2DM has been documented repeatedly, but the mechanism underlying this effect remains largely unknown. The proposed mechanisms include i) weight loss, ii) reduced food intake, and iii) secretion of gut hormones. Diabetes resolution frequently occurs within 10 days post-surgery, long before any significant weight loss. Most researchers do not consider weight loss to be the sole mechanism driving T2DM resolution following the surgery, although significant sustained weight loss does improve long-term insulin resistance. Reduction of food intake occurs immediately post-surgery, which causes in many cases decreased insulin demand and rapid improvement in T2DM. On the other hand, gastric banding (a traditional therapy focused on weight loss through lifestyle change) (Madden *et al*. 2008) and an animal study based on restricted food intake (Pacheco *et al*. 2007) did not result in notable diabetes control. The foregut (Hickey *et al*. 1998), midgut (Troy *et al*. 2008), and hindgut (Thaler & Cummings 2009) hypotheses provide more likely explanations. The midgut hypothesis states that hyperplasia of the Roux-limb *per se* greatly increases glucose consumption. Recent studies increasingly indicate a close connection between glucose homeostasis and the gut (Li *et al*. 2013), and investigation of the effects of bariatric surgery on T2DM will help clarify that connection.

Diabetes develops only in insulin-resistant subjects with pancreatic β-cell defects. Our knowledge of pancreatic β-cell changes following bariatric surgery is fragmentary, but there is some evidence of β-cell recovery. In a clinical study of a large population, Schauer *et al*. (2003) found that patients with less severe T2DM were more likely to achieve complete resolution. Patients whose diabetes did not completely resolve following the surgery typically had the disease for many years. Progressive β-cell failure, which is characteristic of longstanding T2DM, presumably rendered the pathology irreversible in these cases. Results from non-obese Goto-Kakizaki (GK) and streptozotocin (STZ)-treated T2DM rat models undergoing ileal transposition indicated that the procedure reverted irregularly-shaped fibrotic islets to normal phenotype indistinguishable from that of nondiabetic animals (Patriti *et al*. 2007). Duodenal-jejunal bypass also resulted in increased β-cell area and reduced islet fibrosis in GK rats (Speck *et al*. 2011). Studies using a porcine model revealed increased β-cell mass following gastric bypass (Lindqvist *et al*. 2014). Service *et al*. (2005) reported that patients who underwent RYGB surgery were ~400-fold more likely to develop nesidioblastosis (a disease involving pathologic overgrowth of β-cells and life-threatening hypoglycemia), relative to the <0.1% frequency of this disease in the general population. One possibility is that the complication results from increased proliferative activity of β-cells following bariatric surgery, but this idea is controversial. Meier *et al*. (2006) did not find notable changes in fractional β-cell area or β-cell turnover after bypass surgery in patients with hyperinsulinemic hypoglycemia. Histological studies of human pancreases face several obstacles, including wide variation among individuals, limited availability of the organ, and non-availability of data on total pancreatic weight.

In view of the recent trend away from 'bariatric surgery' and toward 'metabolic surgery', we used a non-obese rodent model to study changes in the pancreas following RYGB. To study effects of RYGB independent of weight loss on islets, we performed the surgery on spontaneous T2DM GK rats (GK-GBP), a non-obese model with inherited β-cell deficits. The control groups were i) sham-operated rats pair-fed with the GK-GBP group (termed GK-PF-Sham) and ii) normal Wistar rats. The parameters evaluated and compared among the one experimental and two control groups were islet function, pancreas weight, pancreatic protein and DNA content, centrally located α-cells, pancreatic β-cell fraction, individual β-cell size, β-cell to non-β cell ratio, islet size distribution, small islets closely related to exocrine ducts, and proliferation and apoptosis of β-cells. Elucidation of β-cell changes following RYGB in a non-obese model will help clarify the mechanisms of diabetes remission and lead to possible new strategies for 'metabolic' surgery.

Materials and methods

Animals

Wistar and GK rats from a Japanese colony were obtained from the National Rodent Laboratory Animal Center, Shanghai. Animals were housed in a temperature- and humidity-controlled facility with strict light control. Surgery was performed on 3-month (M)-old GK rats. Oral glucose tolerance tests (OGTT) were performed 1.5 M after

http://joe.endocrinology-journals.org
DOI: 10.1530/JOE-14-0701

Published by Bioscientifica Ltd.

surgery in age-controlled Wistar, GK-PF-Sham, and GK-GBP groups. Animals were sacrificed at age 6 M (i.e. 3 M after surgery). For each of the three groups, i) six pancreases were excised, weighed, and embedded in paraffin blocks for immunohistochemical evaluation; ii) six pancreases were carefully divided into biliary, duodenal, and gastrosplenic portions and frozen at −80 °C for measurement of protein and DNA content; iii) six pancreases were used for *in situ* perfusion experiments. All experiments were approved by the Institutional Animal Care and Use Committee at Shanghai Institutes of Biological Science, China Academy of Science, in compliance with National Institutes of Health (NIH) guidelines and the NIH Guide for the Care and Use of Laboratory Animals.

Surgical procedures

Detailed surgical procedures were described previously (Zhang *et al*. 2013). In brief, RYGB surgery was performed on overnight fasted rats under continuous isoflurane anesthesia. The body of the stomach in rats has a white line indicating the border between the forestomach and glandular stomach. The stomach was carefully divided into two by suture along the white line. Special care was taken at the small curve of the stomach to avoid damaging the left and right gastric arteries and vagus nerve, and to ensure that the upper pouch (white pouch) was continuous with the esophagus. A biliopancreatic limb extending 16 cm from the ligament of Treitz was transected. The distal segment was anastomosed to the gastric remnant, and the proximal segment was drained into 12 cm of the Roux limb by side-to-side anastomosis. For sham-operated animals, the incision was made at a spot 16 cm from the ligament of Treitz. The intestine was then reconnected by side-to-side anastomosis, without intestinal rearrangement, and the incision was closed.

After surgery, animals were left to recover in a warm box and then returned to the animal facility. They were injected with buprenorphine and ampicillin for 3 days. For 12 h following surgery, animals were given only purified water to drink. Standard laboratory chow was provided thereafter.

Pre-weighed pellets were placed in the cage, and recovered food was weighed the next day to calculate 1-day food consumption. The average food consumption of the GK-GBP group was calculated and administered to the GK-PF-Sham group. This procedure was repeated and adjusted once per week.

OGTT and measurements of plasma c-peptide, glucagon like peptide-1, and gastric inhibitory polypeptide

Rats were fasted overnight before OGTT. Glucose load (2 g/kg body weight) was administered orally. Glucose levels were measured from tail bleed with a glucometer (Roche) at 0, 30, 60, and 120 min after glucose administration. One week later, OGTT were repeated with the same glucose load. Blood (0.75 ml) was drawn by eye bleed at 0 and 30 min. For measurement of c-peptide, total glucagon like peptide-1 (GLP-1), and total gastric inhibitory polypeptide (GIP), plasma was evaluated using a corresponding ELISA kit (EMD Millipore, Billerica, MA, USA).

In situ pancreatic perfusion

In situ perfusion of isolated pancreases was performed as described previously (Maechler et al. 2002). In brief, insulin secretion from pancreas was evaluated 3 M post-operation. The pancreas was isolated with the upper part of the duodenum attached, and carefully separated from surrounding tissues (spleen, stomach, colon) by tying and cutting between two sutures. The pancreas with attached duodenum was maintained by perfusion at 5 ml/min. For the initial 20 min, the pancreas was equilibrated at 37 °C in KRB buffer, pH 7.4, supplemented with 10 mmol/l HEPES, 0.1% bovine serum albumin, and 2.8 mmol/l glucose. The perfusate was gassed with a mixture of 95% O_2/5% CO_2 to obtain constant pH and oxygenation. Following the equilibration period, basal effluent was collected for 5 min at 1-min intervals from a catheter placed in the portal vein. Next, the buffer was changed to KRB containing 16.7 mmol/l glucose for 15 min. The complete effluent was collected and frozen at −80 °C for subsequent insulin RIA (EMD Millipore). Area under the curve (AUC) of first-phase insulin secretion (0–4 min) was calculated after subtraction of basal AUC determined during the first 5 min (−5 to −1 min) of fraction collection.

Protein and DNA content of pancreas

Pancreases were divided into biliary, duodenal, and gastrosplenic portions as described by Kara (2005). The biliary portion is located between the biliopancreatic duct and descending duodenum. The duodenal portion is between the biliopancreatic duct and the beginning of the jejunum as marked by the mesoduodenum, which attaches the duodenum to the dorsal abdominal wall. The gastrosplenic portion (the largest portion) continues

http://joe.endocrinology-journals.org
DOI: 10.1530/JOE-14-0701

Published by Bioscientifica Ltd.

along the dorsal aspect of the stomach toward the visceral surface of the spleen and transverse colon. Pancreases were carefully cut without attached fat or vessels by a single experienced researcher, and the three portions were separated by cutting along connecting tissues. Protein and DNA content were measured for the gastrosplenic portion.

For DNA extraction, a TIANamp Genomic DNA kit (Tiangen Biotech, Shanghai, China) was used according to the manufacturer's instructions. DNA was determined by spectrophotometry at 260 and 280 nm (Thermo Nanodrop 2000C).

For protein extraction, tissue from the gastrosplenic portion was immersed in RIPA lysis buffer with protease inhibitors cocktail. The specimen was homogenized by T10 basic Ultra-Turrax (level 4) and shaken on ice (Orbital Shaker 2D-9556-A) for 30 min. The suspension was centrifuged (Eppendorf 5415R; 16.060 ***g***) for 15 min at 4 °C, and supernatant (200 µl) was pipetted into a new tube. A 5-µl sample was vortexed with 45 µl RIPA buffer, and yield was determined by BCA method using Synergy2 ELISA (BioTek, Winooski, VT, USA) and a BCA Protein Assay kit (Thermo. Waltham, MA, USA) according to the manufacturer's instructions.

Morphological and immunohistochemical analyses

Pancreases were carefully excised without attachment of visible other tissues (fat, duodenum, lymph nodes) by an experienced researcher, blotted, positioned in a consistent manner on pre-weighed glass slides, weighed, fixed in 4% paraformaldehyde for 4 h at room temperature, washed, transferred to cassettes, and positioned in the same manner. The fixed tissues were dehydrated in ethanol, cleared in xylene, and embedded in paraffin blocks. Sections (thickness 5 µm) were cut sequentially, mounted on polylysine-coated slides, rehydrated, and subjected to immunohistochemical staining. Antibodies (Abs) used were rabbit primary Ab to insulin (1:400; Cell Signaling, Danvers, MA, USA), goat primary Abs to insulin, glucagon, pancreatic polypeptide, and somatostatin (respectively 1:500, 1:200, 1:200, 1:200; Santa Cruz), mouse primary mAb Ki67 (1:100; Dako; Glostrup, Denmark), FITC-, Cy-, and Alexa-conjugated donkey secondary Abs (1:1000; Jackson Immunoresearch, West Grove, PA, USA). *In situ* apoptosis was detected by TUNEL assay kit (Roche). Nuclei were counterstained with DAPI (1:1000; Cell Signaling).

For determination of β-cell mass, ten sections (at least 200 µm apart) were immunostained with insulin and counterstained with DAPI. In relation to total sections, 1.9% to 2.5% of each pancreas was analyzed. A minimal sample size equal to 1.22% of the total is sufficient to achieve measurement error $<10\%$ (Chintinne *et al*. 2010). Sections were examined using a confocal microscope (A1; Nikon, Tokyo, Japan) connected to a computer with NIS elements software (Nikon). Images (4×, spanning the entire tissue for each slide) were acquired using an X-Y motorized microscope with resolution sufficient to identify single β-cells, and 'stitched together' using the MetaMorph Software program (V.7; Molecular Devices, Sunnyvale, CA, USA). Insulin staining in each section was calculated by MetaMorph then checked manually to remove irrelevant spots or to add β-cells that stained weakly. MetaMorph quantified total tissue area (based on measurement of DAPI-stained area) and insulin-positive area (based on measurement of insulin-stained area) to generate β-cell ratio, which was then multiplied by pancreas weight to obtain β-cell mass. The β-cell/non-β endocrine cell ratio was estimated similarly, as insulin-positive area divided by glucagon/somatostatin/c-peptide cocktail-positive area in ten sections.

For evaluation of islet size distribution, frequency of small size islets related to exocrine ducts, islet structure, and intra-islet α-cell quantification, ten sections 200 µm apart from each rat were stained for glucagon, and counterstained with hematoxylin/eosin (HE) (Beyotime, Shanghai, China). Staining of slides was digitalized using an Olympus IX71 inverted system microscope by scanning the tissue area with 10× objective magnification. To evaluate islet size distribution, all islets in the digital images were measured manually and analyzed using Image Pro Plus Software as described previously (Butler *et al*. 2003, Lamprianou *et al*. 2011). In brief, detectable putative islet-like structures were outlined manually. Diameters of islets in the regions of interest were measured and assigned to three categories: <50 µm, 50–100 µm, and >100 µm. The islet size distribution in each rat was calculated as islet number in each category divided by total islet number encountered. The ratio shown for each experimental group represents mean ± S.E.M. of six animals. Islets related to exocrine ducts were evaluated as described previously (Meier *et al*. 2006). Small islets (diameter <50 µm) in close proximity (<5 nuclei distance from ductal cells) were considered to be positively related to exocrine ducts (Meier *et al*. 2006). The ratio was calculated as number of small islets positively related to ducts divided by total small islet number. For evaluation of islet structure, all putative islet-like structures were checked manually. Normal structure was defined as oval-shaped islets with α-cells present in the mantle. The ratio was calculated as number of islets

http://joe.endocrinology-journals.org
DOI: 10.1530/JOE-14-0701

Published by Bioscientifica Ltd.

with normal structure divided by total islet number encountered. Intra-islet α-cells were quantified as described previously (Chen *et al*. 2013), with slight modification. In brief, islets were grouped according to long diameter, with each 100-μm increment corresponding to a different category. Widths of α-cells were measured by Image Pro Plus, considering islet shape as an ellipse. The distances of α-cells to islet edge in every 100-μm category were calculated. A threshold distance was chosen. Glucagon-positive α-cells whose distance from the islet edge was greater than the threshold value were considered to be interior α-cells. The percentage of interior α-cells calculated by this method was $<5\%$ in Wistar rats. To calculate interior α-cell area in islets of the GK-GBP and GK-PF-Sham groups, each islet was represented as an ellipse based on the short and long diameters of the islet, and the islet was categorized as based previously on the long diameter category. A concentric ellipse was drawn according to the threshold distance of α-cell width. Total α-cell area and interior α-cell area were calculated by Image Pro Plus based on the concentric ellipses. Interior α-cell area was calculated as glucagon-positive staining area within the inner ellipse. The ratio of interior α-cells was calculated as interior α-cell area divided by total α-cell area.

For determination of mean individual β-cell cross-sectional area, five islets per animal were selected at random, and the insulin-positive area of each islet was divided by the number of nuclei within that area (Saisho *et al*. 2013).

For determination of β-cell apoptosis frequency, slides were co-stained with TUNEL and insulin. An average of 1952 ± 24 insulin-positive cells per animal was counted. β-cell apoptosis frequency was calculated as number of apoptotic cells with both TUNEL and insulin-positive staining divided by total number of insulin-positive endocrine nuclei.

Replication measurement was first confirmed in spleen tissue sections. β-cell replication frequency was calculated as number of cells with Ki67 and DAPI co-staining in the nucleus and insulin staining in plasma divided by total number of insulin-positive cells. The two largest slides from sections separated by at least 200 μm were counted.

Statistical

Data were expressed as mean ± S.E.M. Statistical analysis was performed using ANOVA when appropriate, followed by unpaired Student's *t*-test. Differences between means were considered to be significant for $P<0.05$.

Results

Effects of RYGB on metabolic control in non-obese diabetic GK rats

The status of metabolic control in GK rats was evaluated 1.5 M after RYGB surgery. Fasting blood glucose levels at time 0 did not differ significantly between the GK-GBP and GK-PF-Sham groups but glucose levels and AUC of glucose in the GK-GBP group were significantly lower at 120 min, after the oral glucose challenge (Fig. 1A and B). Fasting c-peptide levels at 0 min were significantly lower in the GK-GBP group (Fig. 1C), indicating lower insulin resistance after RYGB. At 30 min, c-peptide levels did not differ significantly among the three groups. However, values of fold insulin response, calculated by dividing c-peptide levels at 30 min by those at 0 min, suggest possible improvement of pancreatic β-cell function after oral glucose load (Fig. 1D).

Levels of incretins (GIP, GLP-1) were measured in blood samples at 0 and 30 min. Basal GIP levels did not differ significantly among the three groups. GIP levels after oral glucose load were significantly lower in GK-PF-Sham than in Wistar. RYGB surgery significantly increased plasma GIP levels after oral glucose gavage (Fig. 1E). The GIP fold response data are consistent with such improvement. Basal GLP-1 levels were significantly higher in GK-GBP than in GK-PF-Sham or Wistar. Similar trends were observed for stimulated GLP-1 levels at 30 min. No GLP-1 increase was seen between 0 and 30 min in GK-PF-Sham. GLP-1 fold changes in GK-GBP and Wistar were significantly higher than in GK-PF-Sham.

To rule out interference of factors such as incretins and insulin action on insulin secretion, we performed *in situ* perfusion of isolated pancreases to evaluate *in vitro* islet function in intact pancreatic blood vessels. The Wistar group showed a typical biphasic pattern of insulin secretion with first phase from 0 to 4 min after switching the perfusion buffer from 2.8 to 16.7 mM glucose (Fig. 2A). Basal insulin levels *in vitro* were significantly lower in GK-GBP and GK-PF-Sham than in Wistar (Fig. 2A and B). Fasting c-peptide levels *in vivo* at 0 min were comparable for GK-PF-Sham vs Wistar, but 2.5-fold lower for GK-GBP vs Wistar (Fig. 1C). The comparison of basal insulin secretion *in vitro* and *in vivo* indicated poor secretion in GK rats after RYGB. After switching to high-glucose perfusion buffer, first-phase insulin secretion was completely lost in GK-PF-Sham. In GK-GBP, a slight but significant increase of first-phase insulin secretion was detected after switching to 16.7 mM glucose (Fig. 2B and C),

http://joe.endocrinology-journals.org
DOI: 10.1530/JOE-14-0701

Published by Bioscientifica Ltd.

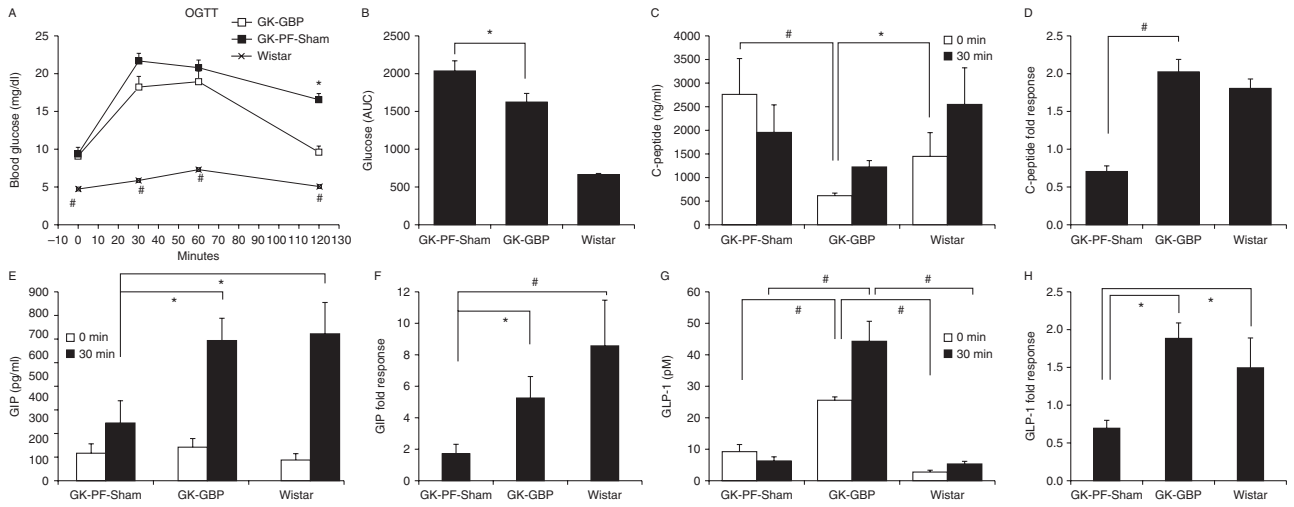

Figure 1

Effects of RYGB on glycemia control, pancreatic β-cell function, and incretin levels after oral glucose load in non-obese diabetic GK rats. (A) Oral glucose tolerance tests (OGTT) were performed in the GK-GBP group 1.5 M after RYGB surgery, and in age-controlled GK-PF-Sham and Wistar groups (each $n=6$). Rats were fasted overnight and then orally administered glucose (2 g/kg body weight). Blood glucose levels were measured at the indicated time points. $^{\#}P<0.01$ vs GK-GBP; $^{*}P<0.05$ vs GK-GBP. (B) AUC of glucose. Levels of C-peptide (C), GIP (E), and GLP-1 (G) at 0 min (white bar) and 30 min (black bar) in the three groups. Mean fold response of C-peptide (D), GIP (F), and GLP-1 (H) calculated as level at 30 min divided by level at 0 min. For (B, C, D, E, F, G and H): $^{\#}P<0.01$; $^{*}P<0.05$; $n=6$.

but the AUC of first-phase insulin response remained much lower than in Wistar (Fig. 2C). Insulin levels show an increasing trend during second-phase insulin response in both GK-PF-Sham and GK-GBP (Fig. 2B).

These findings indicate that glycemic control and β-cell function were improved in the GK rat model 1.5 M after RYGB surgery.

Effects of RYGB on pancreas hyperplasia

Animals were sacrificed 3 M post-surgery. At this time, body weights of the two GK groups were similar (GK-PF-Sham: 351.0±9.2 g; GK-GBP: 351.7±8.9 g; each $n=6$; $P>0.05$). Body weights of the Wistar group (497.5±14.1 g; $n=6$) were significantly ($P<0.01$) higher than those of both GK groups. Pancreas wet weight at time of sacrifice was 1.14±0.04 g in GK-PF-Sham and much higher (1.56±0.06 g) in GK-GBP (Fig. 3A). Pancreas weight expressed as g per 100 g body weight did not differ significantly between Wistar and GK-PF-Sham, but was much higher in GK-GBP (Fig. 3B).

Cellular hypertrophy or hyperplasia is a potential cause of pancreas enlargement. We measured DNA and protein levels in pancreas, because ratios of DNA and

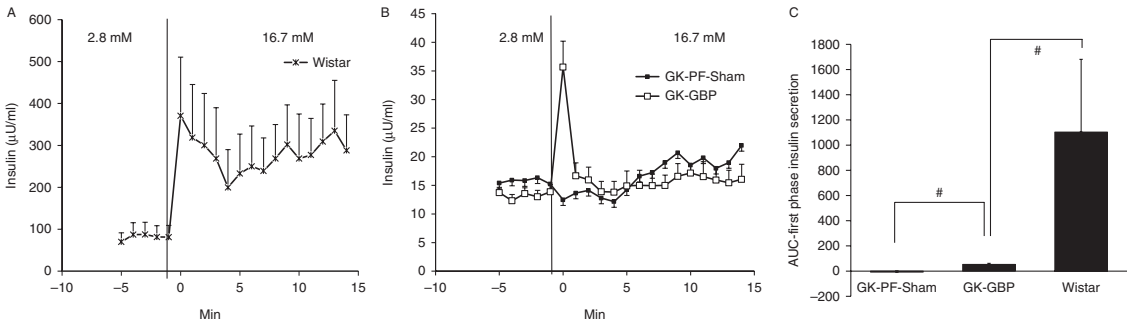

Figure 2

Effects of RYGB on pancreatic β-cell secretion evaluated by *in situ* perfusion of isolated pancreases. Pancreases were isolated and perfused with KRB buffer. Each pancreas was switched from buffer containing 2.8 mM glucose to buffer containing 16.7 mM glucose at −1 min. (A) Insulin secretion from Wistar pancreas. A biphasic insulin response was observed after the switch to high glucose. (B) Insulin secretion from GK-PF-Sham (■) and GK-GBP (□) pancreases. (C) AUC of first-phase insulin secretion (0–4 min) was calculated after subtraction of basal AUC determined during the first 5 min (−5 to −1 min) of fraction collection. $^{\#}P<0.01$; $n=6$.

http://joe.endocrinology-journals.org
DOI: 10.1530/JOE-14-0701

Published by Bioscientifica Ltd.

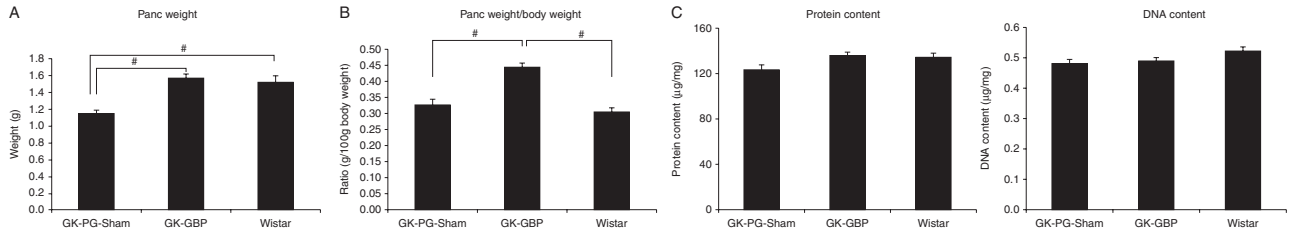

Figure 3
Pancreatic hyperplasia after RYGB in GK rats. (A) Pancreas wet weights in the three groups. (B) Pancreas weight expressed as g per 100 g body weight. (C) Protein and DNA content of gastrosplenic portion of pancreas tissues. Data shown are mean ± S.E.M. $^{\#}P<0.01$; $n=6$.

proteins to equivalent volumes of pancreatic tissues are generally indicative of cellular hypertrophy and hyperplasia (Haegel *et al.* 1981). Protein amount per 100 mg pancreas tissue was similar among the three groups (Fig. 3C, left), indicating that increase of pancreas weight following surgery was not due to increased water content. Ratios of DNA content per 100 mg pancreas tissue were also similar among the three groups, indicating that cellular hyperplasia occurred after surgery (Fig. 3C, right).

Effects of RYGB on islet morphology and β-cell mass

Islet morphology was studied in paraffin-embedded specimens. The Wistar group showed typical islet structure (round or oval shape), with a large proportion of β-cells in the middle and a small proportion of glucagon-positive α-cells in the mantle (Fig. 4A, right). In contrast, islets in GK-PF-Sham showed an irregular pattern with a much higher proportion of α-cells, often found in the central core (Fig. 4A, left). The percentage of islets with normal structure in GK-PF-Sham was 32.0 ± 0.1%. In contrast, the percentage in GK-GBP was 60.5 ± 0.1%, similar to that in Wistar group, and α-cells were located mainly in the islet periphery (Fig. 4A, middle). Measurement of interior α-cell area as a percentage of glucagon-positive area within the inner ellipse, relative to total glucagon-positive area, revealed a significant reduction of interior α-cell area within islets (Fig. 4B).

Analysis of β-cell ratio measured as a percentage of insulin-positive area relative to total pancreas tissue area showed that the value for GK-GBP (1.57 ± 0.1%) was slightly but significantly higher than that for GK-PF-Sham (1.35 ± 0.7%) (each $n=6$; $P<0.05$), corresponding to a ~16% increase of β-cell ratio. The β-cell ratio for Wistar (2.23 ± 0.1%) was significantly ($P<0.01$) higher than that for GK-GBP (Fig. 5A). Total β-cell mass (product of β-cell ratio times pancreas weight) was ~60% higher in GK-GBP (24.6 ± 1.3 mg) than in GK-PF-Sham (15.4 ± 0.8 mg) (Fig. 5B).

The ratio of β-cells to non-β endocrine cells was not notably affected by RYGB surgery (Fig. 5C), indicating that the number and proportion of non-β endocrine cells (predominantly glucagon-positive α-cells) were not reduced. This ratio was much higher ($P<0.01$) in Wistar than in GK-PF-Sham or GK-GBP. β-cell cross-sectional area did not differ significantly among the three groups (Wistar 163 ± 4 µm^2, GK-PF-Sham 171 ± 3 µm^2, GK-GBP 167 ± 4 µm^2; $P>0.05$). These findings are consistent with

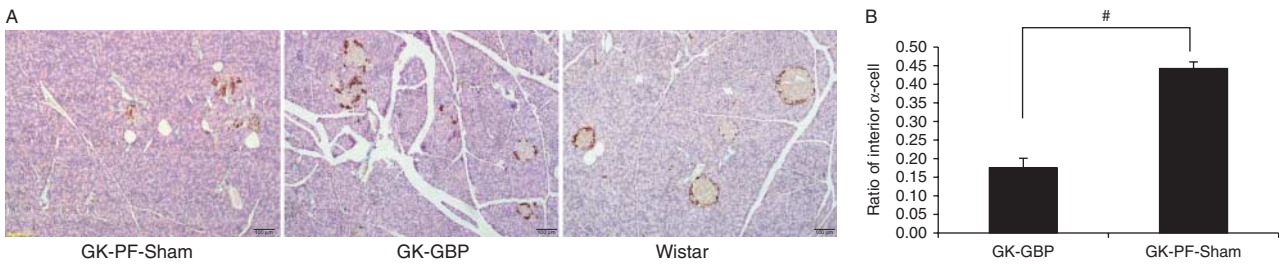

Figure 4
Morphological analysis of islet structure following RYGB in GK rats. (A) Representative microscopy/scanned immunohistology images of islets from the three groups stained with glucagon (dark brown) and counter-stained with HE. (B) Interior α-cell areas for the three experimental groups, calculated as described in Results/'Effects of RYGB on islet morphology and β-cell mass'. $^{\#}P<0.01$; $n=6$. A full colour version of this figure is available at http://dx.doi.org/10.1530/JOE-14-0701.

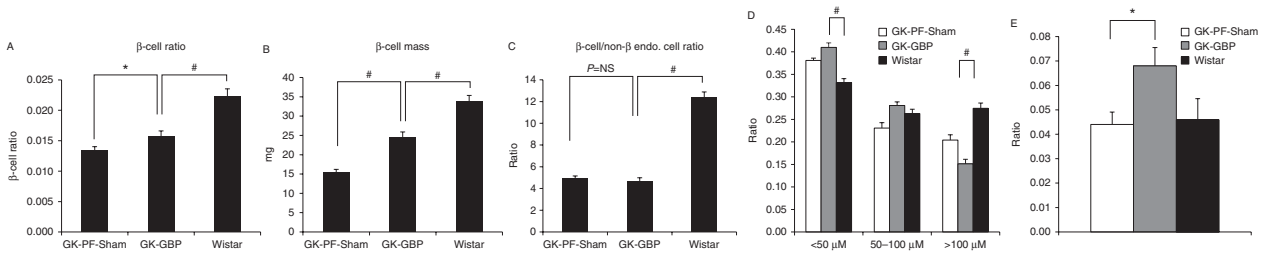

Figure 5

Islet cell morphology and Islet size distribution following RYGB in GK rats. (A) Ten pancreas sections (at least 200 μm apart) were immunostained with insulin and glucagon/somatostatin/c-peptide cocktail, and counterstained with DAPI. Digital images of immunohistochemically stained sections were captured to quantify β-cell ratio as a percentage of insulin-positive area relative to whole pancreas section area. (B) Pancreatic β-cell mass, calculated as β-cell ratio times pancreas weight. (C) Ratio of insulin-positive β-cell to non-β endocrine cell area, estimated as insulin-positive area divided by glucagon/somatostatin/c-peptide cocktail-positive area in ten sections per animal. (D) Islets in the three experimental groups were categorized according to long diameter, and proportions of small islets were calculated, as described in M&M/'Morphological and immunohistochemical analyses'. (E) Small islets (diameter <50 μm) closely related to exocrine ducts were counted, and their proportion relative to total small islets was calculated. Data shown are mean ± S.E.M. $^{\#}P<0.01$; $^{*}P<0.05$; $n=6$.

those for DNA and protein content, and are indicative of islet hyperplasia.

The frequency of β-cell replication, assessed by staining of Ki67 in the nucleus and insulin in the cytoplasm, was very low in all three groups, consistent with previous reports (Meier *et al.* 2008). Frequency of β-cell apoptosis, assessed by staining of TUNEL in the nucleus and insulin in the cytoplasm, did not differ ($P>0.05$) between GK-PF-Sham (0.61 ± 0.07%) and GK-GBP (0.48 ± 0.04%), but was significantly ($P<0.01$) lower in Wistar (0.14 ± 0.07%).

Analysis of islet size distribution showed a significant increase in proportion of small islets (diameter <50 μm) and corresponding decrease in proportion of large islets after gastric bypass surgery, relative to Wistar (Fig. 5D). The proportion of small islets closely related to exocrine ducts was also significantly higher after surgery (Fig. 5E).

Discussion

Type 2 diabetes mellitus (T2DM) develops only in insulin-resistant subjects with β-cell defects. A major challenge in reversing the progressive deterioration of glycemic control over time in T2DM is to increase β-cell mass and promote β-cell function to fulfill the unmet need for insulin. Gastric bypass surgery has been shown to reverse T2DM or block disease progression, leading to diabetes remission in many morbidly obese patients (Pories *et al.* 1995, Hickey *et al.* 1998, Schauer *et al.* 2003, Khoo *et al.* 2014). In the present study, gastric bypass surgery in a non-obese diabetic rodent (GK rat) model led to significant improvement in postprandial hyperglycemia, plasma c-peptide level and first-phase insulin secretion, normalization of islet structure, and increase of β-cell mass with proportional increase of non-β endocrine cells and pancreas tissue hyperplasia. No notable changes in β-cell apoptosis or proliferation were observed following surgery. There was a notable increase in number of small islets closely related to exocrine ducts. These findings clearly highlight changes in the pancreas following gastric bypass surgery in a non-obese T2DM rodent model.

We observed increased pancreatic hyperplasia as a function of body weight following surgery. Associations between changes in the intestine and pancreas have been reported in previous studies. Haegel *et al.* (1981) found that massive resection of the small intestine in rats led to exocrine pancreas hyperplasia. Many studies have addressed the effects of gut hormones on pancreatic hypertrophy and hyperplasia. Cholecystokinin (CCK) (Miyasaka *et al.* 1998, Saillan-Barreau *et al.* 1999) and GLP-1 (Tasyurek *et al.* 2014) exert clear trophic effects on the pancreas. The effect of GLP-1 is presumably related to its impact on β-cell growth (Xu *et al.* 2006). GLP-1-based drugs are becoming increasingly popular in diabetes therapy because they do not cause weight gain or hypoglycemic episodes. The possibility that such drugs may increase the risk of pancreatitis and pancreatic cancer in humans remains controversial (Cohen 2013, Moses 2013). The pancreas tissue hyperplasia observed in our non-obese rat model may have resulted from multiple stimuli related to changes in the gut following RYGB. Some findings from our rat model study suggest a possible link between RYGB and subsequent pancreatic cancer. However, no compelling evidence for such a link has emerged from clinical use of bariatric surgery in humans during the past ~50 years. Kant *et al.* (2011) reported a

http://joe.endocrinology-journals.org
DOI: 10.1530/JOE-14-0701

Published by Bioscientifica Ltd.

40-fold increase in protumorigenic cytokine MIF level following RYGB and raised the question of colorectal neoplastic risk. Long-term clinical studies of neoplastic risk following RYGB are needed to reconcile or resolve observations and controversies along this line. Evaluation of the benefits and risk of RYGB will require more information on long-term outcomes of weight loss, remission or improvement of diabetes, hyperlipidemia, and hypertension (e.g. Buchwald *et al*. 2004), and on nutritional deficiencies, mortality, incidence of cancer and other side effects of bariatric surgery.

Increased β-cell area and decreased islet fibrosis in rodent models (Speck *et al*. 2011) and increased β-cell mass in porcine models (Lindqvist *et al*. 2014) have been reported following various types of bariatric surgery. Surgery *per se* plays a key role in inducing β-cell mass increase in animal models, since food intake and body weight typically remain identical (Patriti *et al*. 2007, Speck *et al*. 2011, Lindqvist *et al*. 2014). Little is known regarding effects of RYGB surgery on β-cell mass in humans. RYGB surgery patients frequently experience postprandial hypoglycemia. Some of these cases are most likely caused by nesidioblastosis (Service *et al*. 2005), while others clearly are not. In a study by Meier *et al*. (2006), pancreases obtained by partial pancreatectomy from six post-gastric bypass patients with hyperinsulinemic hypoglycemia showed no increase of β-cell area, and levels of β-cell neogenesis, replication, and apoptosis were similar to those in controls. A major limitation of most human studies is the impossibility of analyzing the entire pancreas. Instead, β-cell ratio (β-cell area as a percentage of pancreas area) is typically calculated. In the present study, the difference between GK-GBP and GK-PF-Sham groups was exaggerated when β-cell mass, rather than relative β-cell area, was measured (Fig. 5A and B). Non-invasive imaging of pancreatic β-cell mass and function has been applied in normal and diabetic patients (Normandin *et al*. 2012), but the accuracy of this approach needs to be further evaluated. The ratio of β-cells to non-β endocrine cells was unchanged after RYGB in the present study (Fig. 5C), suggesting that gastric bypass surgery results in a significant increase of α-cells. Enhanced fasting glucagon levels and post-surgery glucagon secretion have been observed in animal and human studies (Jorgensen *et al*. 2012, Eickhoff *et al*. 2014). In the present study and others using the GK rat model (Saeidi *et al*. 2013), fasting blood glucose level was not notably altered following RYGB, presumably because of the increase of α-cells and enhancement of fasting glucagon response. Our observation of increased numbers of both α- and?β-cells in combination with improvement of overall glucose metabolism is intriguing. More detailed studies are needed regarding the role of α-cell/β-cell balance in the pathophysiology of T2DM.

Findings of β-cell functional recovery following various types of bariatric surgery are fairly consistent in animal model studies (Hickey *et al*. 1998, Patriti *et al*. 2007, Lindqvist *et al*. 2014), but not with results of human studies. Improved first-phase insulin secretion was reported following i.v. glucose injection in bypass surgery patients (Salinari *et al*. 2013). During isoglycemic i.v. glucose clamping, β-cell function in patients remained significantly impaired in comparison with non-obese control subjects (Dutia *et al*. 2014). In our *in situ* pancreatic perfusion experiment, first-phase insulin secretion was improved in the GK groups, which is encouraging because the major defect of β-cell function in GK rats is first-phase insulin secretion (Oger-Roussel *et al*. 2013). However, both basal and first-phase insulin secretion were still significantly lower than levels in Wistar. Similar first-phase insulin secretion data under pancreatic perfusion were obtained for GK rats treated with GLP-1 during the first postnatal week (Tourrel *et al*. 2002). β-cell function during oral glucose load in the first postnatal week was normalized in bypass surgery patients (Dutia *et al*. 2014), consistent with our c-peptide results following oral glucose challenge. These findings demonstrate the importance of the gastrointestinal system in regulation of metabolism.

The reasons for increased β-cell ratio (measured as percentage insulin-positive area relative to total pancreas tissue area) and β-cell mass after RYGB are also unclear. Increased numbers of total small islets and of small islets related to exocrine ducts have been considered to reflect islet neogenesis (Xu *et al*. 2006). However, findings in transgenic mice suggest that new β-cells arise from existing β-cells (Dor *et al*. 2004). Recent studies indicate that β-cells may dedifferentiate under metabolic stresses (Talchai *et al*. 2012), and that insulin therapy can cause redifferentiation of dedifferentiated β-cells (Wang *et al*. 2014). RYGB surgery resulting in β-cell redifferentiation may also lead to increased β-cell ratio and mass, as observed in our animal model. Detailed investigation of this possibility is underway. Further elucidation of the mechanisms responsible for surgery-induced islet improvement and its relationship with pancreatic hyperplasia will greatly enhance our understanding of T2DM pathogenesis, and facilitate development of novel agents for T2DM therapy.

http://joe.endocrinology-journals.org
DOI: 10.1530/JOE-14-0701

Published by Bioscientifica Ltd.

Declaration of interest
The authors declare that there is no conflict of interest that could be perceived as prejudicing the impartiality of the research reported.

Funding
This study was supported by the Major State Basic Research Development Program of China 973 (grant no. 2011CB504003), National Natural Science Foundation of China (grant nos 81471047, 81070657, and 61134013), National High-Tech R&D Program of China 863 (no. 2012AA020406), and NN-CAS Research Foundation (no NNCAS-PostDoc-2011-1). The authors are grateful to Dr S Anderson for English editing of the manuscript.

Author contribution statement
C Y and H Z designed the research; X Z, B Q, C L, and L J conducted the research; L J, Z L, and B L analyzed the data; X Z, L J, and H Z wrote the manuscript. All the authors read and approved the final manuscript.

Acknowledgements
We thank Dr Pierre Maechler for demonstrating to us his advanced techniques for *in situ* pancreatic perfusion.

References

Buchwald H, Avidor Y, Braunwald E, Jensen MD, Pories W, Fahrbach K & Schoelles K 2004 Bariatric surgery: a systematic review and meta-analysis. *Journal of the American Medical Association* **292** 1724–1737. (doi:10.1001/jama.292.14.1724)

Butler AE, Janson J, Bonner-Weir S, Ritzel R, Rizza RA & Butler PC 2003 β-cell deficit and increased β-cell apoptosis in humans with type 2 diabetes. *Diabetes* **52** 102–110. (doi:10.2337/diabetes.52.1.102)

Chen H, Martin B, Cai H, Fiori JL, Egan JM, Siddiqui S & Maudsley S 2013 Pancreas++: automated quantification of pancreatic islet cells in microscopy images. *Frontiers in Physiology* **3** 482. (doi:10.3389/fphys.2012.00482)

Chintinne M, Stangé G, Denys B, In 't Veld P, Hellemans K, Pipeleers-Marichal M, Ling Z & Pipeleers D 2010 Contribution of postnatally formed small β cell aggregates to functional β cell mass in adult rat pancreas. *Diabetologia* **53** 2380–2388. (doi:10.1007/s00125-010-1851-4)

Cohen D 2013 Hyperplasia from GLP-1 drugs is 'not a surprise,' say researchers. *BMJ* **346** f2025. (doi:10.1136/bmj.f2025)

Dor Y, Brown J, Martinez OI & Melton DA 2004 Adult pancreatic β-cells are formed by self-duplication rather than stem-cell differentiation. *Nature* **429** 41–46. (doi:10.1038/nature02520)

Dutia R, Brakoniecki K, Bunker P, Paultre F, Homel P, Carpentier AC, McGinty J & Laferrère B 2014 Limited recovery of β-cell function after gastric bypass despite clinical diabetes remission. *Diabetes* **63** 1214–1223. (doi:10.2337/db13-1176)

Eickhoff H, Louro T, Matafome P, Seica R & Castro e Sousa F 2014 Glucagon secretion after metabolic surgery in diabetic rodents. *Journal of Endocrinology* **223** 255–265. (doi:10.1530/JOE-14-0445)

Haegel P, Stock C, Marescaux J, Petit B & Grenier JF 1981 Hyperplasia of the exocrine pancreas after small bowel resection in the rat. *Gut* **22** 207–212. (doi:10.1136/gut.22.3.207)

Hickey MS, Pories WJ, MacDonald KG Jr, Cory KA, Dohm GL, Swanson MS, Israel RG, Barakat HA, Considine RV, Caro JF *et al.* 1998 A new paradigm for type 2 diabetes mellitus: could it be a disease of the foregut? *Annals of Surgery* **227** 637–643. (doi:10.1097/00000658-199805000-00004)

Jorgensen NB, Jacobsen SH, Dirksen C, Bojsen-Moller KN, Naver L, Hvolris L, Clausen TR, Wulff BS, Worm D, indqvistHansen D *et al.* 2012 Acute and long-term effects of Roux-en-Y gastric bypass on glucose metabolism in subjects with type 2 diabetes and normal glucose tolerance. *American Journal of Physiology-Endocrinology and Metabolism* **303** E122–E131. (doi:10.1152/ajpendo.00073.2012)

Kant P, Sainsbury A, Reed KR, Pollard SG, Scott N, Clarke AR, Coletta PL & Hull MA 2011 Rectal epithelial cell mitosis and expression of macrophage migration inhibitory factor are increased 3 years after Roux-en-Y gastric bypass (RYGB) for morbid obesity: implications for long-term neoplastic risk following RYGB. *Gut* **60** 893–901. (doi:10.1136/gut.2010.230755)

Kara ME 2005 The anatomical study on the rat pancreas and its ducts with emphasis on the surgical approach. *Annals of Anatomy* **187** 105–112. (doi:10.1016/j.aanat.2004.10.004)

Khoo CM, Muehlbauer MJ, Stevens RD, Pamuklar Z, Chen J, Newgard CB & Torquati A 2014 Postprandial metabolite profiles reveal differential nutrient handling after bariatric surgery compared with matched caloric restriction. *Annals of Surgery* **259** 687–693. (doi:10.1097/SLA.0b013e318296633f)

Lamprianou S, Immonen R, Nabuurs C, Gjinovci A, Vinet L, Montet XC, Gruetter R & Meda P 2011 High-resolution magnetic resonance imaging quantitatively detects individual pancreatic islets. *Diabetes* **60** 2853–2860. (doi:10.2337/db11-0726)

Li B, Zhou X, Wu J & Zhou H 2013 rom gut changes to type 2 diabetes remission after Gastric Bypass Surgeries. *Frontiers of Medicine* **7** 191–200. (doi:10.1007/s11684-013-0258-2)

Lindqvist A, Spégel P, Ekelund M, Garcia Vaz E, Pierzynowski S, Gomez MF, Mulder H, Hedenbro J, Groop L & Wierup N 2014 Gastric bypass improves β-cell function and increases β-cell mass in a porcine model. *Diabetes* **63** 1665–1671. (doi:10.2337/db13-0969)

Madden SG, Loeb SJ & Smith CA 2008 An integrative literature review of lifestyle interventions for the prevention of type II diabetes mellitus. *Journal of Clinical Nursing* **17** 2243–2256. (doi:10.1111/j.1365-2702.2008.02335.x)

Maechler P, Gjinovci A & Wollheim CB 2002 Implication of glutamate in the kinetics of insulin secretion in rat and mouse perfused pancreas. *Diabetes* **51** S99–102. (doi:10.2337/diabetes.51.2007.S99)

Meier JJ, Butler AE, Galasso R & Butler PC 2006 Hyperinsulinemic hypoglycemia after gastric bypass surgery is not accompanied by islet hyperplasia or increased β-cell turnover. *Diabetes Care* **29** 1554–1559. (doi:10.2337/dc06-0392)

Meier JJ, Butler AE, Saisho Y, Monchamp T, Galasso R, Bhushan A, Rizza RA & Butler PC 2008 β-cell replication is the primary mechanism subserving the postnatal expansion of β-cell mass in humans. *Diabetes* **57** 1584–1594. (doi:10.2337/db07-1369)

Miyasaka K, Ohta M, Tateishi K, Jimi A & Funakoshi A 1998 Role of cholecystokinin-A (CCK-A) receptor in pancreatic regeneration after pancreatic duct occlusion: a study in rats lacking CCK-A receptor gene expression. *Pancreas* **16** 114–123. (doi:10.1097/00006676-199803000-00002)

Moses A 2013 Novo Nordisk replies to BMJ investigation on incretins and pancreatic damage. *BMJ* **347** f4386. (doi:10.1136/bmj.f4386)

Normandin MD, Petersen KF, Ding YS, Lin SF, Naik S, Fowles K, Skovronsky DM, Herold KC, McCarthy TJ, Calle RA *et al.* 2012 *In vivo* imaging of endogenous pancreatic β-cell mass in healthy and type 1 diabetic subjects using 18F-fluoropropyl-dihydrotetrabenazine and PET. *Journal of Nuclear Medicine* **53** 908–916. (doi:10.2967/jnumed.111.100545)

Oger-Roussel S, Behr-Roussel D, Caisey S, Kergoat M, Charon C, Audet A, Bernabé J, Alexandre L & Giuliano F 2013 Bladder and erectile dysfunctions in the Type 2 diabetic Goto-Kakizaki rat. *American Journal of Physiology Regulatory, Integrative and Comparative Physiology* **306** R108–R117. (doi:10.1152/ajpregu.00033.2013)

Pacheco D, de Luis DA, Romero A, González Sagrado M, Conde R, Izaola O, Aller R & Delgado A 2007 The effects of duodenal-jejunal exclusion on

Published by Bioscientifica Ltd.

hormonal regulation of glucose metabolism in Goto-Kakizaki rats. *American Journal of Surgery* **194** 221–224. (doi:10.1016/j.amjsurg.2006.11.015)

Patriti A, Aisa MC, Annetti C, Sidoni A, Galli F, Ferri I, Gullà N & Donini A 2007 How the hindgut can cure type 2 diabetes. Ileal transposition improves glucose metabolism and β-cell function in Goto-Kakizaki rats through an enhanced proglucagon gene expression and L-cell number. *Surgery* **142** 74–85. (doi:10.1016/j.surg.2007.03.001)

Pories WJ, Swanson MS, MacDonald KG, Long SB, Morris PG, Brown BM, Barakat HA, deRamon RA, Israel G, Dolezal JM *et al.* 1995 Who would have thought it? An operation proves to be the most effective therapy for adult-onset diabetes mellitus *Annals of Surgery* **222** 339–352. (doi:10.1097/00000658-199509000-00011)

Saeidi N, Meoli L, Nestoridi E, Gupta NK, Kvas S, Kucharczyk J, Bonab AA, Fischman AJ, Yarmush ML & Stylopoulos N 2013 Reprogramming of intestinal glucose metabolism and glycemic control in rats after gastric bypass. *Science* **341** 406–410. (doi:10.1126/science.1235103)

Saillan-Barreau C, Dufresne M, Clerc P, Sanchez D, Corominola H, Moriscot C, Guy-Crotte O, Escrieut C, Vaysse N, Gomis R *et al.* 1999 Evidence for a functional role of the cholecystokinin-B/gastrin receptor in the human fetal and adult pancreas. *Diabetes* **48** 2015–2021. (doi:10.2337/diabetes.48.10.2015)

Saisho Y, Butler AE, Manesso E, Elashoff D, Rizza RA & Butler PC 2013 β-cell mass and turnover in humans: effects of obesity and aging. *Diabetes Care* **36** 111–117. (doi:10.2337/dc12-0421)

Salinari S, Bertuzzi A, Guidone C, Previti E, Rubino F & Mingrone G 2013 Insulin sensitivity and secretion changes after gastric bypass in normotolerant and diabetic obese subjects. *Annals of Surgery* **257** 462–468. (doi:10.1097/SLA.0b013e318269cf5c)

Schauer PR, Ikramuddin S, Gourash W, Ramanathan R & Luketich J 2000 Outcomes after laparoscopic Roux-en-Y gastric bypass for morbid obesity. *Annals of Surgery* **232** 515–529. (doi:10.1097/00000658-200010000-00007)

Schauer PR, Burguera B, Ikramuddin S, Cottam D, Gourash W, Hamad G, Eid GM, Mattar S, Ramanathan R, Barinas-Mitchel E *et al.* 2003 Effect of laparoscopic Roux-en Y gastric bypass on type 2 diabetes mellitus. *Annals of Surgery* **238** 467–484. (doi:10.1097/01.sla.0000089851.41115.1b)

Scopinaro N, Gianetta E, Adani GF, Friedman D, Traverso E, Marinari GM, Cuneo S, Vitale B, Ballari F, Colombini M *et al.* 1996 Biliopancreatic diversion for obesity at eighteen years. *Surgery* **119** 261–268. (doi:10.1016/S0039-6060(96)80111-5)

Service GJ, Thompson GB, Service FJ, Andrews JC, Collazo-Clavell ML & Lloyd RV 2005 Hyperinsulinemic hypoglycemia with nesidioblastosis after gastric-bypass surgery. *New England Journal of Medicine* **353** 249–254. (doi:10.1056/NEJMoa043690)

Speck M, Cho YM, Asadi A, Rubino F & Kieffer TJ 2011 Duodenal-jejunal bypass protects GK rats from β-cell loss and aggravation of hyperglycemia and increases enteroendocrine cells coexpressing GIP and GLP-1. *American Journal of Physiology-Endocrinology and Metabolism* **300** E923–E932. (doi:10.1152/ajpendo.00422.2010)

Talchai C, Xuan S, Lin HV, Sussel L & Accili D 2012 Pancreatic β cell dedifferentiation as a mechanism of diabetic β cell failure. *Cell* **150** 1223–1234. (doi:10.1016/j.cell.2012.07.029)

Tasyurek HM, Altunbas HA, Balci MK & Sanlioglu S 2014 Incretins: their physiology and application in the treatment of diabetes mellitus. *Diabetes Metabolism Research and Reviews* **30** 354–371. (doi:10.1002/dmrr.2501)

Thaler JP & Cummings DE 2009 Minireview: hormonal and metabolic mechanisms of diabetes remission after gastrointestinal surgery. *Endocrinology* **150** 2518–2525. (doi:10.1210/en.2009-0367)

Tourrel C, Bailbe D, Lacorne M, Meile MJ, Kergoat M & Portha B 2002 Persistent improvement of type 2 diabetes in the Goto-Kakizaki rat model by expansion of the β-cell mass during the prediabetic period with glucagon-like peptide-1 or exendin-4. *Diabetes* **51** 1443–1452. (doi:10.2337/diabetes.51.5.1443)

Troy S, Soty M, Ribeiro L, Laval L, Migrenne S, Fioramonti X, Pillot B, Fauveau V, Aubert R, Viollet B *et al.* 2008 Intestinal gluconeogenesis is a key factor for early metabolic changes after gastric bypass but not after gastric lap-band in mice. *Cell Metabolism* **8** 201–211. (doi:10.1016/j.cmet.2008.08.008)

Wang Z, York NW, Nichols CG & Remedi MS 2014 Pancreatic β cell dedifferentiation in diabetes and redifferentiation following insulin therapy. *Cell Metabolism* **19** 872–882. (doi:10.1016/j.cmet.2014.03.010)

Wittgrove A & Clark G 2000 Laparoscopic gastric bypass. Roux-en-Y 500 patients: technique and results, with 3-60 month follow-up. *Obesity Surgery* **10** 233–239. (doi:10.1381/096089200321643511)

Xu G, Kaneto H, Lopez-Avalos M, Weir G & Bonner-Weir S 2006 GLP-1/exendin-4 facilitates β-cell neogenesis in rat and human pancreatic ducts. *Diabetes Research and Clinical Practice* **73** 107–110. (doi:10.1016/j.diabres.2005.11.007)

Zhang R, Yan C, Zhou X, Qian B, Li F, Sun Y, Shi C, Li B, Saito S, Horimoto K *et al.* 2013 Association of Rev-erbα in adipose tissues with Type 2 diabetes mellitus amelioration after gastric bypass surgery in Goto-Kakizaki rats. *American Journal of Physiology Regulatory, Integrative and Comparative Physiology* **305** R134–R146. (doi:10.1152/ajpregu.00520.2012)

Received in final form 14 September 2015
Accepted 18 September 2015
Accepted Preprint published online 14 October 2015

http://joe.endocrinology-journals.org
DOI: 10.1530/JOE-14-0701

Published by Bioscientifica Ltd.